NWRI CONTRIBUTION 86-121
Engel (49)
DeZeeuw (13)

IMPROVEMENTS TO THE LOW SPEED RESPONSE OF THE PLASTIC ROTOR FOR THE PRICE CURRENT METER - PHASE II

by

P. Engel[1], K. Wiebe[2], C. DeZeeuw[3], R. Terzi[4]

[2]Head
[4]Standards Officer
Hydrometric Methods and Development Section
Water Survey of Canada
Water Resources Branch
Place Vincent Massey
Hull, Quebec

[1]Research Engineer
Environmental Hydraulics Section
[3]Head, Technical Services Section
Hydraulics Division
National Water Research Institute
Canada Centre for Inland Waters
Burlington, Ontario, Canada L7R 4A6
November 1986

SUMMARY

This study is a joint initiative of Water Survey of Canada and the Hydraulics Division of the National Water Research Institute. Its purpose is to develop a plastic rotor for the Price meter with the best possible low speed performance. Preliminary designs have been obtained based on theoretical considerations and preliminary towing tank tests. Indications are that threshold velocities of less than 2 cm/s can be obtained. Extensive tests were conducted to evaluate the consistency in the performance of the new rotor designs over a wider range of conditions. Results indicate that a plastic rotor with improved response characteristics has been obtained.

MANAGEMENT PERSPECTIVE

Water Survey of Canada intends to convert to plastic rotors for the Price Current Meter to cut down production costs and improve quality control. The improvements in rotor design as a result of this study will lower the threshold velocity for the Price meter, making it a more reliable instrument where flow velocities are small.

Acting Chief
Hydraulics Division

SOMMAIRE

La présente étude est une initiative conjointe des Relevés hydrologiques du Canada et de la Division de l'hydraulique de l'Institut national de recherche sur les eaux. Elle a pour but de mettre au point un rotor de plastique pour le moulinet hydrométrique Price afin d'obtenir le meilleur rendement possible à faible vitesse. Les formes préliminaires ont été élaborées d'après des notions théoriques et à la lumière d'essais dans un bassin d'essai de carènes. On a constaté qu'on peut atteindre des vitesses limites d'entraînement de moins de 2 cm/s. Des essais exhaustifs ont été effe tués pour évaluer l'uniformité de rendement du nouveau rotor dans des conditions plus variées. Les résultats portent à croire que le nouveau rotor possède de meilleures caractéristiques de réponse.

PERSPECTIVE-GESTION

Les Relevés hydrologiques du Canada comptent munir tous les moulinets hydrométriques Price de rotors en matière plastique dans le but de réduire les coûts de production et d'améliorer le contrôle de la qualité. Les améliorations techniques du nouveau rotor résultant de cette étude font que la vitesse limite d'entraînement du moulinet est moins élevée de sorte que l'instrument sera plus fiable pour les mesures de faibles débits.

Le chef intérimaire

Division de l'hydraulique

TABLE OF CONTENTS

1.0 INTRODUCTION

The Price Current Meter is the instrument used by the Water Survey of Canada (WSC) to measure stream flow velocities. The rotor of the conventional Price meter consists of an assembly of six conical cups oriented about the vertical axis of rotation and is attached to the frame of the meter as shown schematically in Figure (1). Traditionally, the rotor components have been fabricated out of sheet brass with the whole assembly being protected with chrome or nickel plating, Figure (2a). Recently, because of production costs and quality control of this type of rotor, the United States Geological Survey (USGS) has introduced a plastic rotor which can be mass-produced more cheaply, precisely, and quickly using plastic injection moulds, Figure (2b). The WSC wants to adopt a similar strategy and is in the process of developing the necessary mould.

Before designing the mould, the writers attempted to modfify the geometry of the conical elements of the USGS rotor in the hope of improving the low speed performance. Such an improvement, if it can be economcally incorporated into the mould design, would ensure a better return for the money invested in the mould. Three modifications of the original rotors geometry were presented by Engel et al. (1985) as shown in Figure 3. Rotor P-3 and P-4 were selected for more intensive testing. The tests were conducted in the towing tank at the National Water Research Institute, Burlington, Ontario. The results are presented in this report.

This report is a continuation of the work originally conducted in 1981 under study number 2203 to evaluate and optimize the performance of the Price Meter Rotor for use under winter flow conditions.

2.0 REVIEW OF ROTOR DESIGN CONSIDERATIONS

The rotor of the Price meter is an assembly of six conical elements mounted symmetrically about the vertical axis of rotation. The forces which govern the rotation of the rotor are the drag forces on the inside and outside of the cups as well as the resistance due to bearings, gears and contacts in the rotor assembly. These forces create torques about the centre of rotation as shown in Figure 4.

For a general turbulent flow with a uniform time averaged velocity distribution as shown in Figure 4, the unbalanced torque acting on the rotor about its axis of rotation at any time t, may be expressed as

$$T_1 - T_2 - T_f = I \frac{dw}{dt} \qquad (1)$$

where T_1 = the torque exerted on the rotor in the direcion of the flow, T_2 = the torque exerted on the rotor in the direction opposite to that of the flow, T_f = the torque exerted on the rotor shaft by bearings, gears and contacts, I = moment of inertia of the rotor, w = angular speed of the rotor and t = time. The moment of inertia of a body of mass m may be expressed as

$$I = mk^2 \qquad (2)$$

where k = radius of gyration of the body which is the distance from the axis of rotation to a point at which the total mass of the body might be concentrated without changing its moment of inertia. Also, for a given rotor geometry and mass, it was shown by Engel et al. (1985), that the rate of rotation of the rotor at a given constant speed, depended on the difference between the torques T_1 and T_2. Taking this differences as

$$\Delta T = T_1 - T_2 \qquad (3)$$

then together with Equations (1) and (2) one may write

$$\Delta T - T_f = mk^2 \frac{dw}{dt} \qquad (4)$$

To improve the rotor's performance, it is desirable to increase its rate of rotation for a given speed of flow in the low speed range and to reduce the frictional resistance. In addition, in order to properly measure turbulent flow, the rotor should be responsive to speed fluctuations as a result of turbulent eddies.

The rate of rotation of the rotor can be increased by increasing ΔT in Equation (4). This can be done by changing the rotor geometry to increase C_{D_1} and decrease C_{D_2} which are the drag coefficients corresponding to the drag forces creating torques T_1 and T_2. Such a change was achieved with the design of rotors P-3 and P-4 as shown in Figure 3. The fricitonal torque T_f can be reduced by reducing the submerged weight of the rotor, thereby reducing the pivot friction of the rotor shaft. The original USGS plastic rotor is heavier in air than the conventional metallic rotor but its submerged weight is less (Table 1). Therefore, the plastic rotor represents an improvement in reducing T_f. However, with the present material used there is no significant reduction in the submerged weight of the new rotors P-3 and P-4 relative to that of the USGS plastic rotor (Table 1). Therefore, the present design modifications do not result in a further reduction of the frictional torque T_f. Finally, the responsiveness of the rotor to turbulent flow has been reduced (dw/dt decreased) by changing from the conventional metallic rotor to the plastic rotor, because the mass of the plastic rotor is greater (Table 1). The responsiveness of the plastic rotor has been further reduced by the designs of rotor P-3 and P-4 because of an increase in mass of 20% and 9% respectively. However, this problem can be reduced by using a lighter material to mold the rotors.

The original USGS rotor and the proposed rotors P-3 and P-4 have been tested extensively in the towing tank at the National Water Research Institute. Using at least three copies of each rotor to assess the repeatability of the rotors' behaviour, tests were conducted with the meters aligned parallel to the direction of travel in the towing tank. One copy of each rotor type was used to determine the effect of meter misalignment to the flow direction, both in the horizontal and vertical plane.

3.0 EXPERIMENTAL EQUIPMENT AND PROCEDURE

3.1 Meter Suspension

The rotors were tested using a Price winter type current meter yoke which was secured to a 20 mm diameter solid steel rod. The assembly was fastened to the rear of the towing carriage. The meters were set and fixed at different angles in the horizontal and vertical direction, using the procedures given by Engel and DeZeeuw (1978, 1979).

3.2 Towing Tank

The tank, constructed of reinforced concrete, founded on piles, is 122 metres long and 5 metres wide. The full depth of the tanks is 3 metres, of which 1.5 metres is below ground level. Normally, the water depth is maintained as 2.7 metres. Concrete was chosen for its stability, vibration reduction and to reduce possible convection currents.

At one end of the tank is an overflow weir. Waves arising from towed current meters and their suspensions are washed over the crest, reducing wave reflections. Parallel to the sides of the tank, perforated beaches serve to dampen laterlal surface wave disturbances. The large cross section of the tank also reduces the generation of waves by the towed object.

3.3 Towing Carriage

The carriage is 3 metres long, 5 metres wide, weighs 6 tonnes and travels on four precision machined steel wheels.

The carriage is operated in three overlapping speed ranges:

0.5 cm/sec - 6.0 cm/sec
5.0 cm/sec - 60 cm/sec
50 cm/sec - 600 cm/sec

The maximum speed of 600 cm/sec can be maintained for 12 seconds. Tachometer generators connected to the drive shafts emit a voltage signal proportional to the speed of the carriage. A feedback control system uses these signals as input to maintain the constant speed within specified tolerances.

3.4 Data Acquisition

3.4.1 Towing speed

The average speed data for the towing carriage is obtained by recording voltage pulses emitted from a measuring wheel. This wheel is attached to the frame of the towing carriage and travels on one of the towing tank rails, emitting a pulse for each millimeter of travel. The frequency of these pulses is measured using a SBC-100 computer which may in the maximum case store 95000 observations for a given run. The average towing speed computed from this data is accurate to within ±0.1% at the 99% confidence level (Engel, 1985).

3.4.2 Rate of revolution of the rotor

The Price meter is equipped with a contact closure mechanism which gives a voltage pulse for each complete revolution of the rotor. The pulses generated by the rotor are transmitted to a data

acquisition module which begins counting the revolutins after the first pulse has been received. This ensures that all the pulses counted represent complete revolutions. In order to obtain the rate of rotation of the rotor in revolutions per second, time is measured simultaneously with the counting of the revolutions using a crystal clock.

3.5 Meter Preparation

Prior to testing, the meter underwent the following inspection:

a) the pentagear was checked to ensure that it was operating freely;
b) the contact wire was cleaned and adjusted for tension to provide good contact;
c) all moving parts were lubricated.

Following the inspection, the meter was hung in a wind tunnel where it was spun for two hours to ensure that all moving parts were "run-in".

3.6 Meter Position

On each test the meter was attached to the rod suspension and lowered into position 30 cm below the water surface. This depth was chosen to avoid surface effects and to create a minimum of drag on the steel suspension rod, thereby reducing undue vibration. In all cases the suspended meter was placed near the centre-line of the towing tank in accordance with test conditions set out by Engel (1977).

3.7 Towing Tests

A tow of the meter with the towing carriage at a pre-set speed was defined as a test. To begin a set of tests, the meter was

properly aligned in the specified position. The meter was then towed at different speeds, resulting in a total of about 50 tests up to a maximum of 400 cm/s. Each time the meter was towed, care was taken that steady state conditions prevailed when measurements were recorded. The lengths of the waiting time between successive tests were in accordance with criteria established by Engel and DeZeeuw (1977) or better. For each test, the towing speed, revolutions of the meter rotor, and time were recorded. Water temperatures were not noted since temperature changes during the tests were small and do not affect the meter significantly (Engel, 1976). At least three rotors of each of the USGS, P-3 and P-4 types were tested with their orientation parallel to the flow with the axis of rotation being normal to the horizontal plane. This orientation was fixed at $\theta = 0°$ and $\alpha = 0°$ (θ = horizontal angle, α = vertical angle). Tests were also conducted on one rotor of each type at angles of 5°, 10°, 15°, 30°, and 45° left and right of $\theta = 0°$ and above and below $\alpha = 0°$. Because the data are very extensive, they are not tabulated in this report but can be made available upon request.

To determine the threshold velocities, the rotors were set at the normal orientation ($\theta = 0°$, $\alpha = 0°$) and each test was begun by towing the meter at a speed which was slower than that required to move the rotor. The towing speed was then increased in small increments, each time allowing conditions to stabilize and observing the behaviour of the rotor. The speed was increased in this way until the rotor was just turning at a constant rate. This was taken to be the threshold velocity. Ten such tests were conducted for one of each of the three rotor models and the average was taken as the representative threshold velocity. The data for these tests are given in Tables 2, 3 and 4 for the USGS, P-3 and P-4 models respectively.

4.0 DATA ANALYSIS

4.1 Response Curves at $\theta = 0°$

The data for the rotors set at $\theta = 0°$ were plotted as N/V vs V in Figure 5 for the USGS, P-3 and P-4 models. In the case of the USGS model, four rotors were used, whereas for the P-3 and P-4 models three rotors were rated. This change in procedure was necessary because one of the original rotors was damaged during the modifications from the original USGS version to the P-3 model. In order to facilitate comparisons, average curves were drawn through the plotted points. This effectively reduced the analysis to considerations of the dominant deterministic response of each rotor by removing the small random component. These average curves were then used to compare the effects of the rotor modifications. In all three cases, the average curve represents the data of the rotor groups very well.

The curve in Figure 5(a) for the USGS rotor shows an increase in N/V with increasing V until when $V = V_c \approx 50$ cm/s (V_c = speed at which N/V becomes constant) at N/V = 1.33. The value of $V_c = 50$ cm/s is smaller than the value of $V_c = 100$ cm/s observed for this rotor type by Engel et al. (1985), for a single rotor, although the value of N/V = 1.33 is the same. The present value of $V_c = 50$ cm/s is based on consistent results obtained with four rotors indicating that there may have been some small physical difference in the single rotor used by Engel et al. (1985).

In Figure 5(b) the curve for rotor P-3 shows the effect of the streamlined noses, while keeping the flat bases of the original conical elements untouched. The curve shows that a reduction in the value of V_c is achieved with this modification, resulting in V_c = 20 cm/s at a value of $N/V \approx 1.32$. In comparing this curve with that of the USGS rotor in Figure 5(a), it can be seen that there is no significant change in N/V. The fact that N/V did not change is contrary to expectations. Data by Hoerner (1965) showed that by changing the conical elements for their given h/d ratio (h = height of

conical element from base to apex, d = diameter of element base) to parabolic solids of revolution, a significant reduction in the drag resistance on the rotor elements could be obtained which in turn should result in an increase in N/V. However, it appears that due to the complex flow patterns around the rotor elements as a result of their close proximity to each other and the rotational motions, the effect on N/V has been neutralized for speeds below 20 cm/s. Nevertheless, the curve in Figure 5(b) shows that the streamlined noses have achieved an improvement in the low speed response by reducing V_c from 50 cm/s to 20 cm/s.

Finally, in Figure 5(c), the average curve shows the combined effect of the shallow depressions and the streamlined noses. The value of V_c, however, is about the same as that for model P-3 in Figure 5(b), although the value of N/V has been icnreased by about two percent to 1.35. On the whole, the improvement obtained with the depressions in the bases of the conical elements is marginal and does not offer a significant improvement over that of model P-3. Considering that rotor model P-4 is much more difficult to produce than model P-3, then the latter would provide the best alternative to the USGS model, providing an improved low speed response when the meters are properly aligned in the flow.

4.2 Effect of Horizontal Departure from True Alignment

To determine the effects of horizontal alignment only one rotor from each of the three models was selected. This was deemed to be sufficient because the angular effects on the rotors are considered to be of secondary importance.

The calibration data for angles to the right of $\theta = 0°$ were plotted as N/V vs V in Figure 6 for the case of true alignment ($\theta = 0°$) and angles of 5°, 10°, 15°, 30° and 45° respectively. The plotted data in Figures 6(a), 6(b), and 6(c) clearly show that the effect of angular alignment to the right is greatest on the original USGS rotor,

whereas the P-3 model is affected least, especially for angles of 30° or less. Indeed, for angles of 15° or less model P-3 is virtually unaffected and only slightly at angles of 30°. This fact bodes well for the P-3 design.

The data for angles to the left of $\theta = 0°$ are plotted as N/V vs V in Figure 7 for the same angles as in Figure 6. The plots clearly show that all three rotor models are less affected by angles to the left than by angles to the right. The best performance is obtained with model P-4, which shows only a small effect of changing the angle of alignment for all angles tested. In the case of model P-3 the results are about the same for $V > 40$ cm/s, although the mean value of N/V is slightly lower at N/V = 1.32 for model P-3 versus N/V = 1.35 for model P-4. However, in the speed range $10 < V < 40$ the response of the P-3 rotor is somewhat irratic with values of N/V ranging from about 1.21 for angles of 10° and 15° to N/V = 1.32 for the remaining angles which is the same as observed for $V > 40$ cm/s. The data for the USGS model show a slightly greater sensitivity to changes in alignment than the P-3 and P-4 models as evidenced by the wider spread of plotted points for $V > 10$ cm/s.

4.3 Effect of Vertical Departure from True Alignments

To determine the effects of vertical alignment once again only one rotor was chosen from each of the three models tested.

The calibration data for angles α above the horizontal plane were plotted as N/V vs V in Figure 8 for the case of true alignment ($\alpha = 0°$) and angles of 5°, 10°, 15°, 30° and 45° respectively. In all cases the horizontal angled θ was set at 0°. The plotted data in Figures 8(a), 8(b), and 8(c) show that all three rotor models are affected by changing the angles above the horizontal plane. For angles of 15° and less, the USGS model is affected more than models P-3 and P-4, while the effect on the models P-3 and P-4 is about the same. For angles of 30°, model P-3 is better than the USGS model and

model P-4 is the best. For angles of 45° there is little difference between the USGS model and model P-3, and again model P-4 is the least affected.

The data for angles below the horizontal plane were plotted as N/V vs V in Figure 9 for the same angles as in Figure 8. The plots clearly show that all the three rotor models are similarly affected by angles above and below the horizontal plane. Once again for angles of 15° and less, both model P-3 and P-4 are less affected by changes in angles than the USGS model, and that P-4 model is best. However in Figure 9(b) the behaviour of the P-3 model is much more favourable relative to the USGS model than was the case for angles above the horizontal plane. For angles of 30° and 45°, the P-3 model is marginally better than the USGS model, whereas the P-4 model is significantly better than the P-3 model.

4.4 Threshold Velocity

One of the improvements in the low speed performance sought with the new rotor designs is a significant reduction in the threshold velocity. This velocity, say V_o, is defined as the minimum velocity at which the rotor will revolve at a constant rate. Near the threshold velocity changes in submerged weight (Engel, DeZeeuw, 1984) are probably more important than changes in geometry made to the original USGS rotor. The data in Tables 1, 2 and 3 show the threshold velocities for the USGS model, P-3 and P-4 models respectively. These results are contrary to what was originally observed by Engel et al., (1985) who found these values to be 3.5 cm/s, 2.0 cm/s and 1.5 cm/s for the USGS models, P-3 and P-4, respectively. Part of the reason for this difference may be attributed to the fact that the results of Engel et al. (1985) were single values only, whereas the present results in Tables 1, 2, and 3 represent averages of ten carefully conducted tests. It is not clear why the threshold velocities for the three rotor models should vary in this way since, the submerged

weights are not much different. It is possible that the differences may be due to such effects as internal gear friction and contact resistance which may have changed slightly when the rotor models were changed in the meter assembly. At any rate, the differences are small, and the threshold velocity of the P-3 and P-4, models are only slightly different from that of the USGS rotor. It is not likely, that for a mechanical meter such as the Price meter, threshold velocities can be reduced much further. Therefore, all three rotor models can be considered to have an excellent threshold velocity for a meter of this type. Some improvement may be obtained by replacing the mechanical/electrical contacts with a fibre optics system to reduce internal friction.

4.5 Linear Regression Equations

It is the present practice to perform linear regressions on the calibration data to obtain calibration equations of the form

$$V = a + bN \quad \ldots\ldots\ldots \quad (5)$$

where "a" is an intercept and "b" is the slope of the equation. Theoretically, if the meter behaves like an ideal meter for which $V_0 = 0$, then $a = 0$. However, because of friction in the bearings and contacts, $V_0 > 0$ and thus the value of "a" depends largely on the magnitude of V_0. However, "a" is always less than V_0 so that $a/V_0 < 1$. As V_0 becomes smaller one expects "a" to become smaller but this also depends on the slope "b" of the equation. Regression equations for the three rotor models being considered were obtained together with their coefficient of correlation "r", and standard error of estimate S_E. These equations are given in Table 5.

For the USGS model, in each case of the four rotors tested, the data could be fitted by a single equation in accordance with the calibration methods presently used by the Water Survey of Canada. In

all cases, the coefficient of correlation are high at 0.999 and the standard errors of estimate vary over the narrow range of 0.51 cm/s to 0.63 cm/s, which may be due to meter characteristics, etc.

Examination of the regression equations for the P-3 rotor model, shows that for two out of the three curves, a single equation was sufficient. However, for the other curve two equations were required. Once again, the correlation coefficients were 0.999 and the standard errors of estimate for the single equation were 0.60 cm/s and 0.65 cm/s which is of the same order as those obtained for the four equations of the USGS model. In the single case where two equations were required for the P-3 model, the values of S_E were considerably lower at 0.45 cm/s and 0.49 cm/s.

Finally, for the P-4 rotor model, the data set for each of the three rotors had to be fitted with two equations, each of which had a high correlation coefficient of 0.999. However, in each case the standard errors of estimate varied from 0.21 cm/s to 0.26 cm/s for the lower range equations, while for the upper speed range equations values of S_E ranged from 0.55 cm/s to 0.58 cm/s. The latter values are of the same order as those obtained with the USGS rotor and hence do not represent any improvement. In contrast to this the values of S_E for the low speed range equations represent a considerable reduction in variance reflecting slightly better consistency in the rotor response in the lower speed range, that is $V \leq 230$ cm/s. However, the reduction in S_E with the P-4 rotor model is not a sufficient improvement to warrant its preference over the P-3 model. The values of S_E for the P-3 rotor may also be reduced by changing the curve fitting procedure, and possibly changing the data point distribution (Engel 1985).

5.0 CONCLUSIONS

1. Development of rotor models P-3 and P-4 using the same plastic as that of the USGS rotor has resulted in an increase of rotor mass

of 20% and 9% respectively. The increase in mass increases each rotor's moment of inertia and tend to reduce its responsiveness to turbulence of the flow. This effect can be counteracted by using lighter plastics.

2. The responses of the USGS P-3 and P-4 rotor models to the different conditions for which they were tested were ranked in order of preference as shown below.

Rotor Type	Rotor Response Ranking				
	$\theta = 0°$ $\alpha = 0°$	Angles Rt. $\alpha = 0°$	Angles Lt. $\alpha = 0°$	Angles Above Hor. $\theta = 0°$	Angles Below Hor. $\theta = 0°$
USGS P-1	3	3	3	3	3
P-3	1	1	2	2	2
P-4	2	2	1	1	1

1 = BEST,

3. The threshold velocities obtained with the three rotor models ranged from 1.6 cm/s to 2.0 cm/s. These results indicate that because of internal gear and contact resistance this is the best that can be achieved regardless of changes in geometry of the rotors.
4. Linear regression equations fitted to the calibration data showed that the P-4 model had the lowest standard error of estimate for speeds less than about 200 cm/s. The standard errors of estimate for the USGS and P-3 models for speeds less than 200 cm/s were similar but larger than that for the P-4 rotor. For speeds greater than 200 cm/s all three rotor types had approximatley the same standard errors of estimate.
5. It may be possible to reduce standard errors of estimate by improving the curve fitting procedure.

6. Tests should be conducted on the moulded rotors of the chosen design to determine consistency of calibration and the effects of changing the mass (i.e., using lighter plastics).

ACKNOWLEDGEMENTS

The authors are grateful to C. Bil and B. Near who conducted the tests and produced the regression equations.

REFERENCES

Engel, P. 1976. A Universal Calibration Equation for Price Meters and Similar Instruments. Scientific Series No. 65, Inland Waters Directorate, CCIW, Burlington, Ontario.

Engel P. and C. DeZeeuw. 1977. Determination of Waiting Times Between Successive Runs When Calibrating Price 622AA Type Current Meters in a Towing Tank. Technical Note, Hydraulics Research Division, Canada Centre for Inland Waters, Burlington Ontario.

Engel, P. and C. DeZeeuw. 1978. The Effect of Horizontal Alignment on the Performance of the Price 622 AA Current Meter. Unpublished Manuscript, Hydraulics Division, NWRI.

Engel, P. and C. DeZeeuw. 1979. The Effect of Vertical Alignment on the Performance of the 622 AA Price Current Meter. Unpublished Manuscript, Hydraulics Division, NWRI.

Engel, P. 1977. An Experimental Outline to Study the Performance of the Price Current Meter. Unpublished Manuscript, Hydraulics Research Division, CCIW, Burlington, Ontario.

Engel, P. and C. DeZeeuw. 1984. On the Effect of Changes in Geometry and Submerged Weight of the Price Meter Rotor. Unpublished Manuscript, Hydraulics Division, NWRI, Burlington, Ontario.

Engel, P. 1985 Calibration of Current Meters for Turbine Efficiency Tests. Unpublished Manuscript, Hydraulics Division, National Water Research Institute, Burlington, Ontario.

Engel, P. K. Wiebe, R. Terzi, and C. DeZeeuw. 1985. Improvements to the Low Speed Response of the Plastic Rotor for the Price Curent Meter - Phase 1. Unpublished Manuscript, Hydraulics Division, NWRI.

Hoerner, S.F. 1965. Fluid-Dynamic Drag. Published by the Author, Library of Congress Catalogue Card Number 64-19666, U.S.A.

TABLE 1

Weights of Rotors in Air and Water

Rotor	Weights in Air (Newtons)	Weight in Water (Newton)
Metallic	1.48	1.29
USGS (P-1)	1.98	0.52
(P-3)	2.40	0.57
(P-4)	2.16	0.57

TABLE 2

Threshold Velocity for USGS Model

Run No.	Velocity (m/s)
1	0.0152
2	0.0201
3	0.0152
4	0.0152
5	0.0152
6	0.0152
7	0.0202
8	0.0152
9	0.0152
10	0.0152
Mean	0.0162

TABLE 3

Threshold Velocity for P-3 Model

Run No.	Velocity (m/s)
1	0.02030
2	0.02030
3	0.01756
4	0.01756
5	0.01755
6	0.01757
7	0.01752
8	0.02030
9	0.02030
10	0.01756
Mean	0.01865

TABLE 4

Threshold Velocity for P-4 Model

Run No.	Velocity (m/s)
1	0.02027
2	0.02028
3	0.02030
4	0.02029
5	0.02031
6	0.02038
7	0.02029
8	0.02030
9	0.02037
10	0.02029
Mean	0.02029

TABLE 5

Regression Equations

Rotor Type	Slope,"b" cm/rev	Intercept,"a"	SE cm/s	r	Speed Range cm/s
USGS #1	74.76	0.49	0.63	0.999	$2.0 \leq V \leq 400$
P-1					
#2	74.94	0.80	0.56	0.999	$2.0 \leq V \leq 400$
#3	74.83	0.78	0.51	0.999	$2.0 \leq V \leq 400$
#4	74.81	0.84	0.55	0.999	$2.0 \leq V \leq 400$
P-3 #1	74.69	0.50	0.60	0.999	$2.0 \leq V \leq 400$
#2	74.80	0.78	0.45	0.999	$2.0 \leq V \leq 204$
	73.12	5.36	0.49	0.999	$2.0 \leq V \leq 400$
#4	74.41	1.02	0.65	0.999	$2.0 \leq V \leq 400$
P-4 #1	72.71	0.74	0.26	0.999	$2.0 \leq V \leq 207$
	70.95	5.73	0.55	0.999	$2.07 \leq V \leq 400$
#2	72.73	0.53	0.21	0.999	$2.0 \leq V \leq 229$
	69.98	9.14	0.55	0.999	$2.29 \leq V \leq 400$
#4	73.12	0.60	0.22	0.999	$2.0 \leq V \leq 180$
	70.96	5.91	0.58	0.999	$1.80 \leq V \leq 400$

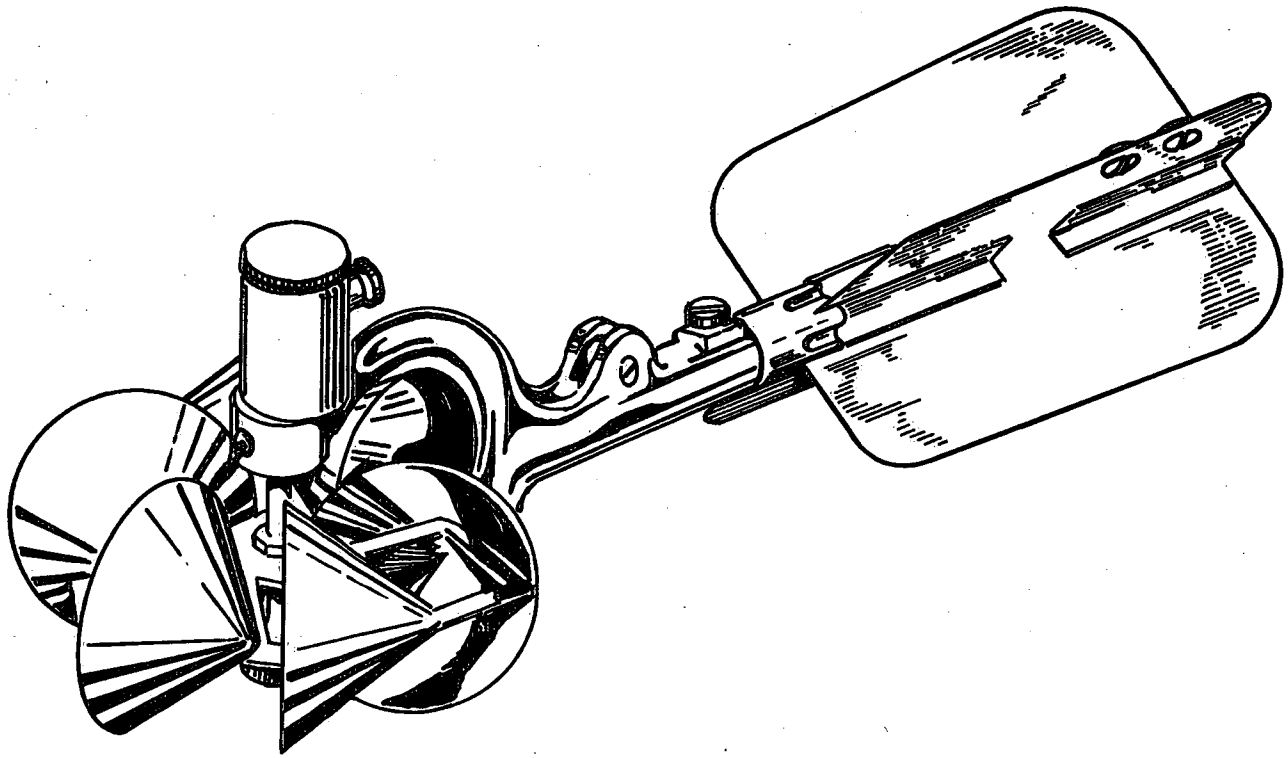

FIGURE 1. PRICE METER WITH CONVENTIONAL ROTOR

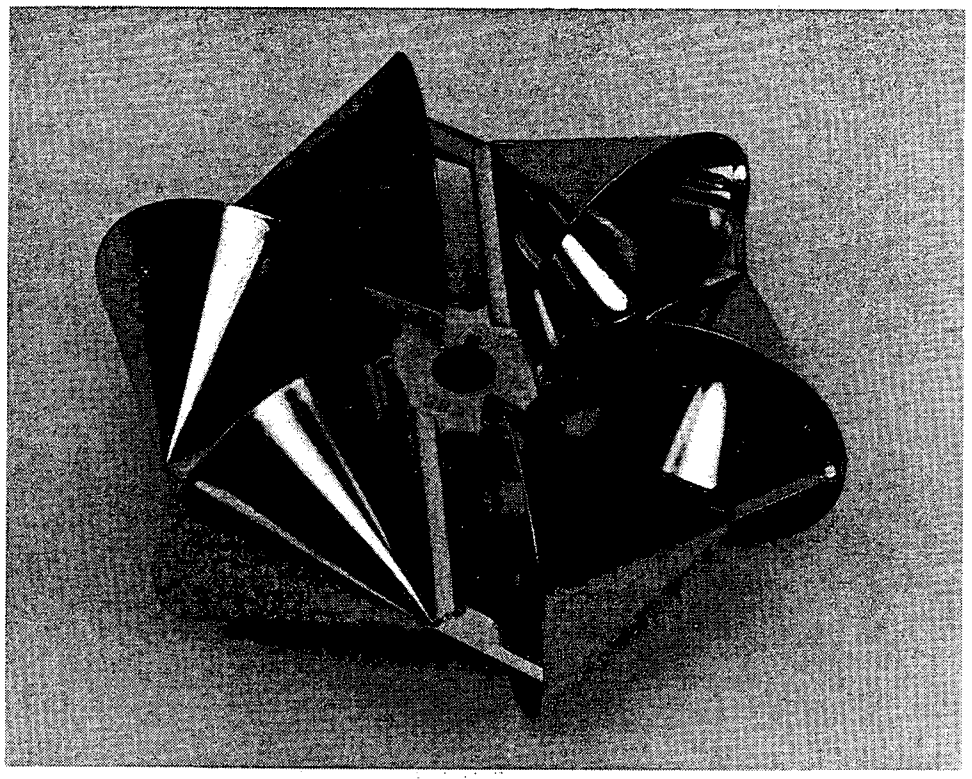

FIGURE 2a. CONVENTIONAL ROTOR

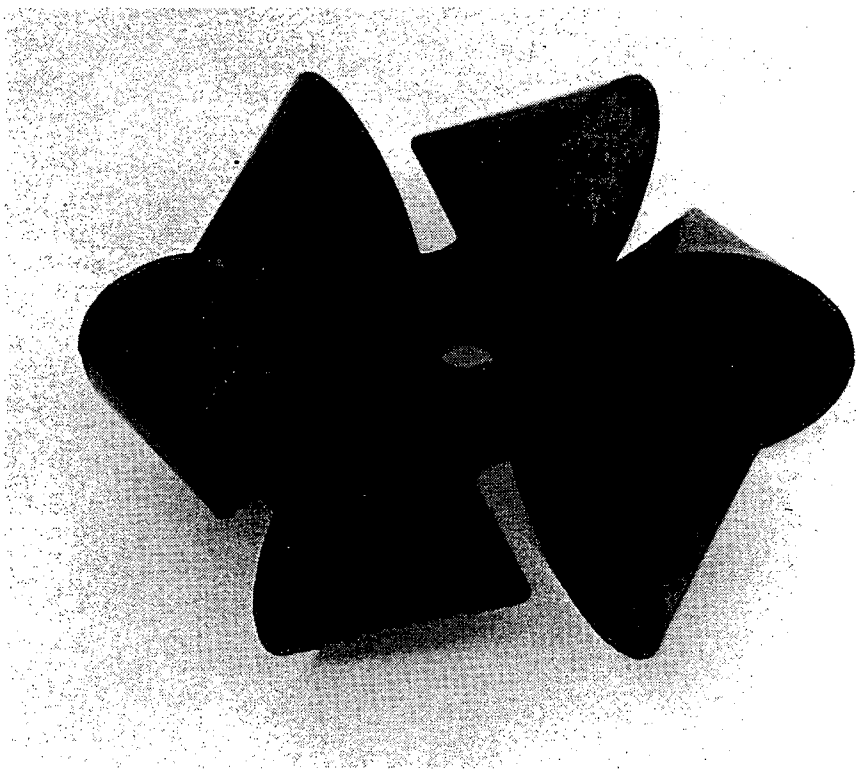

FIGURE 2b. PLASTIC ROTOR

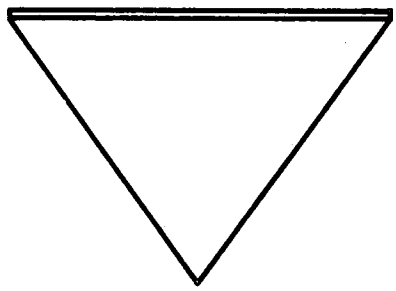

a) ROTOR P-1
(U.S.G.S.)

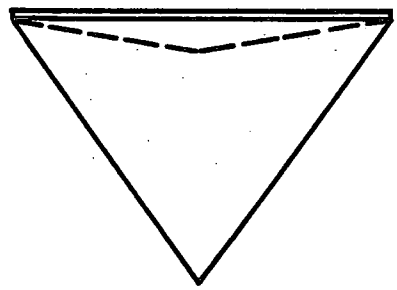

b) ROTOR P-2

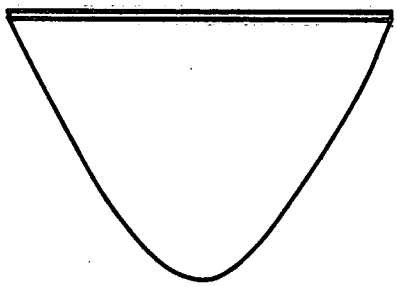

c) ROTOR P-3

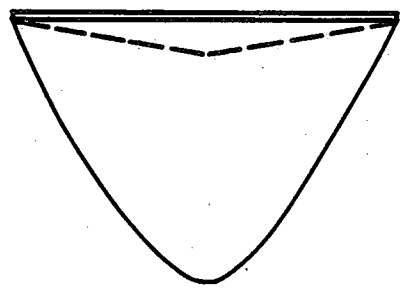

d) ROTOR P-4

Figure 3 Shapes of Rotor Elements Tested
By Engel et al. (1985)

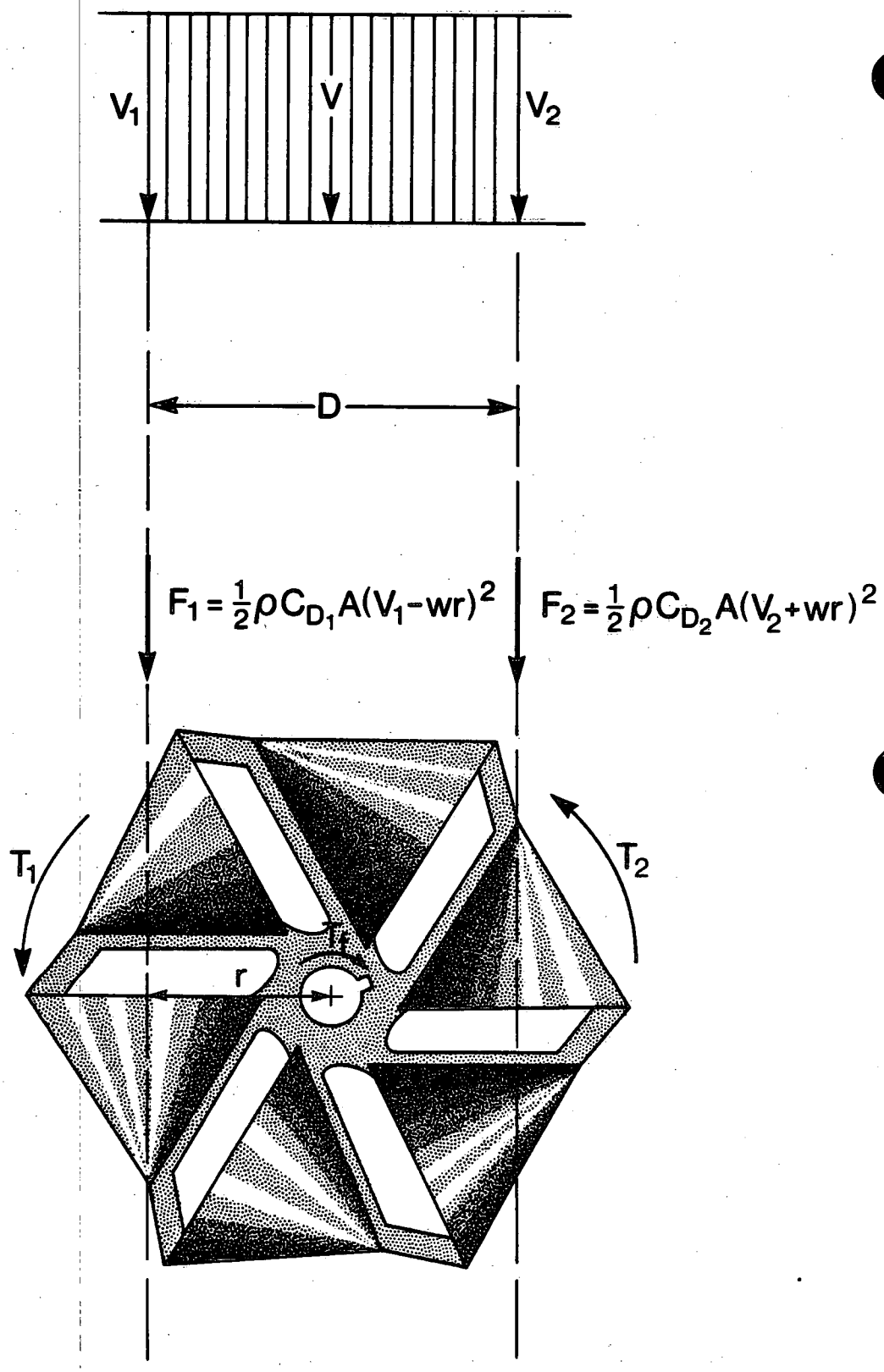

Fig. 4 TORQUES AND VELOCITY DISTRIBUTION FOR TWO DIMENSIONAL FLOW.

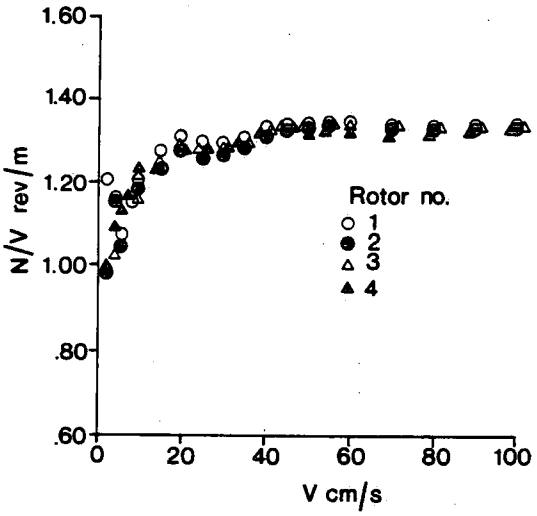

(a) U.S.G.S. (P-1) Rotor

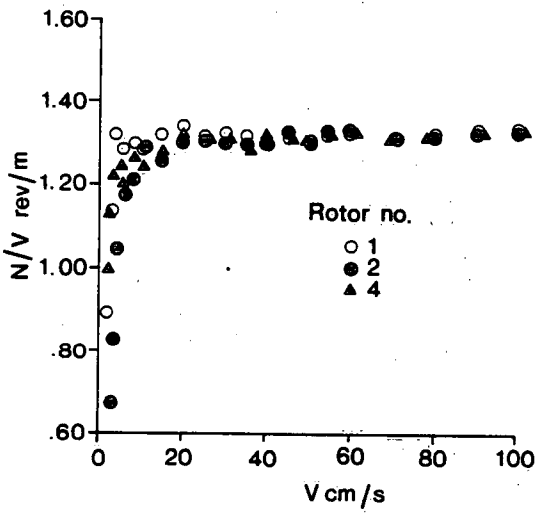

(b) Rotor (P-3)

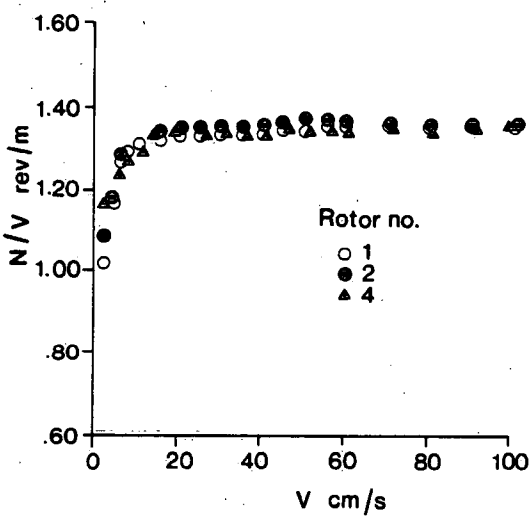

(c) Rotor (P-4)

Fig.5 ROTOR RESPONSE FOR METERS ALIGNED PARALLEL TO TOWING DIRECTION.

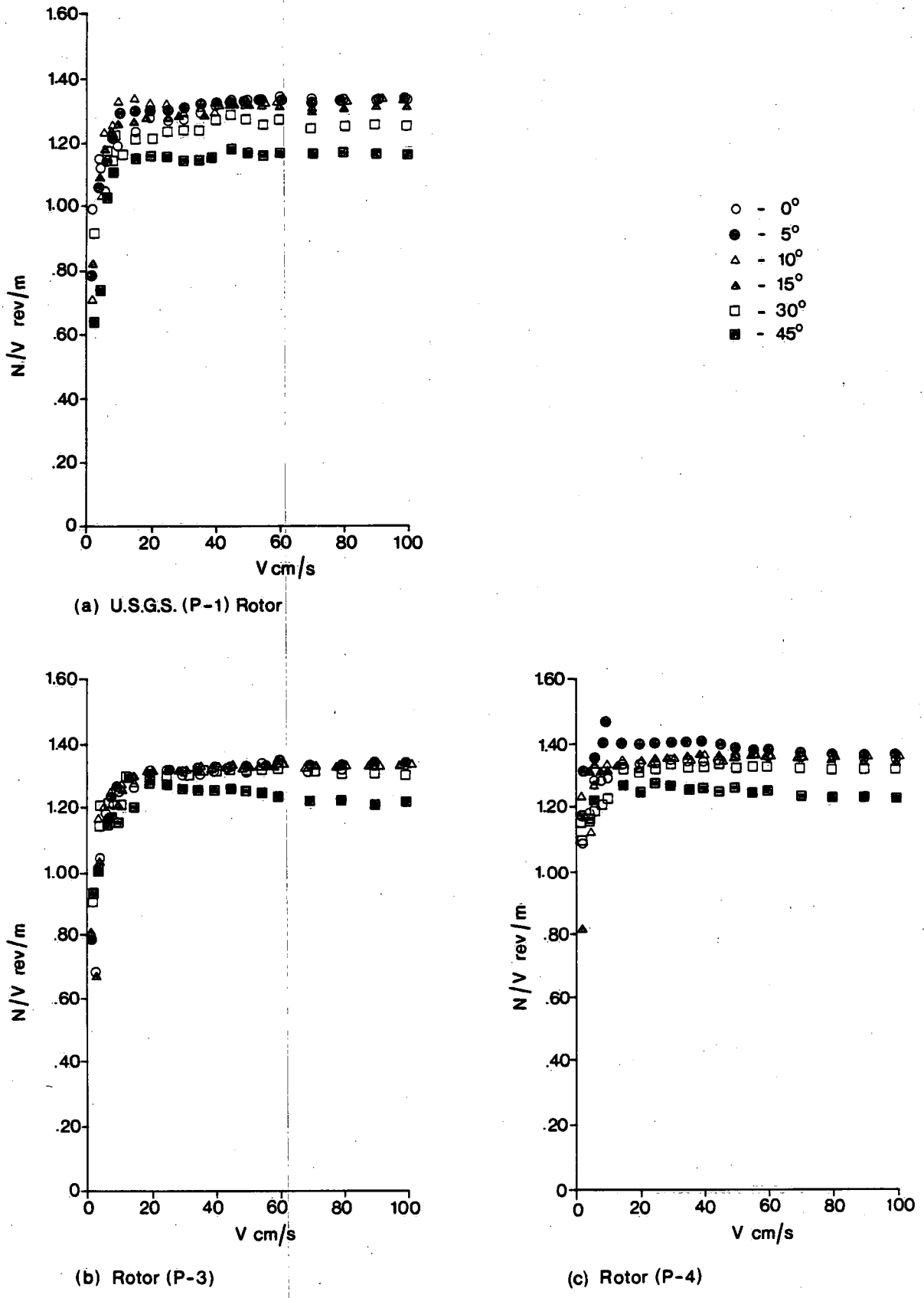

(a) U.S.G.S. (P-1) Rotor

(b) Rotor (P-3)

(c) Rotor (P-4)

Fig. 6 ROTOR RESPONSE FOR METER ANGLES TO THE RIGHT OF TRUE ALIGNMENT

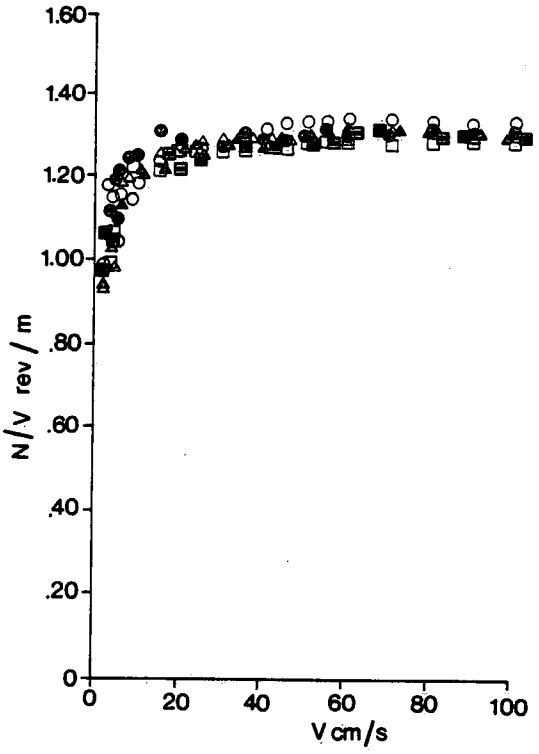

(a) U.S.G.S. Rotor (P-1)

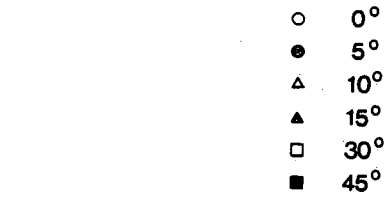

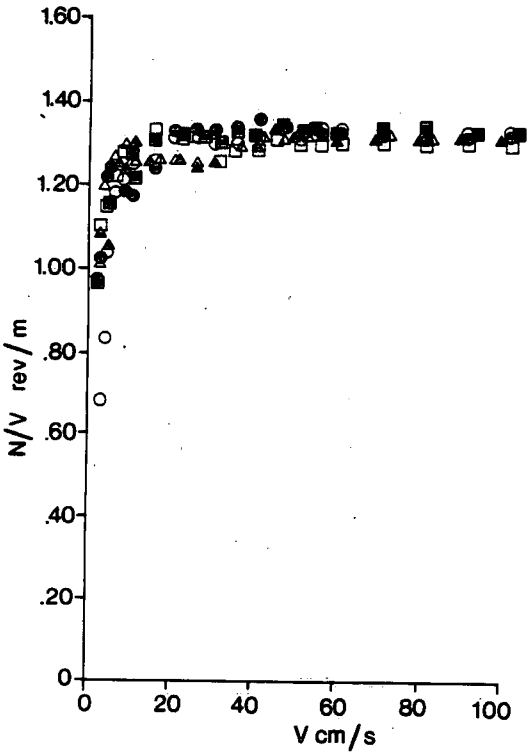

(b) Rotor (P-3)

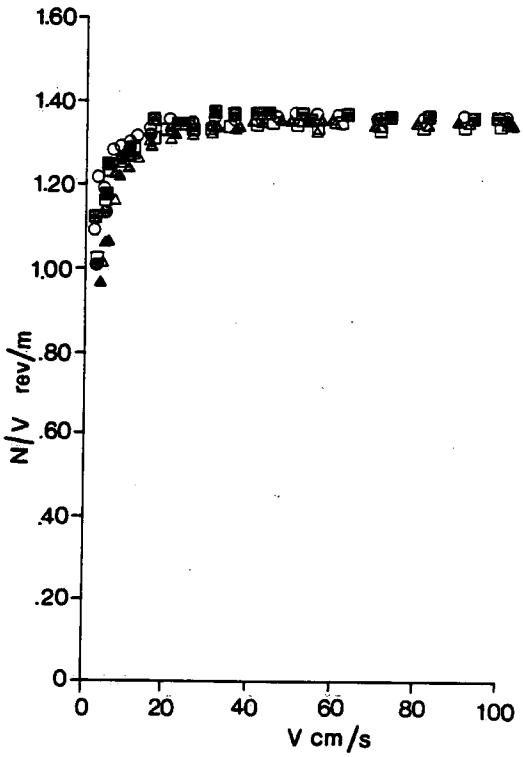

(c) Rotor (P-4)

Fig.7 ROTOR RESPONSE FOR METER ANGLES TO THE LEFT OF TRUE ALIGNMENT.

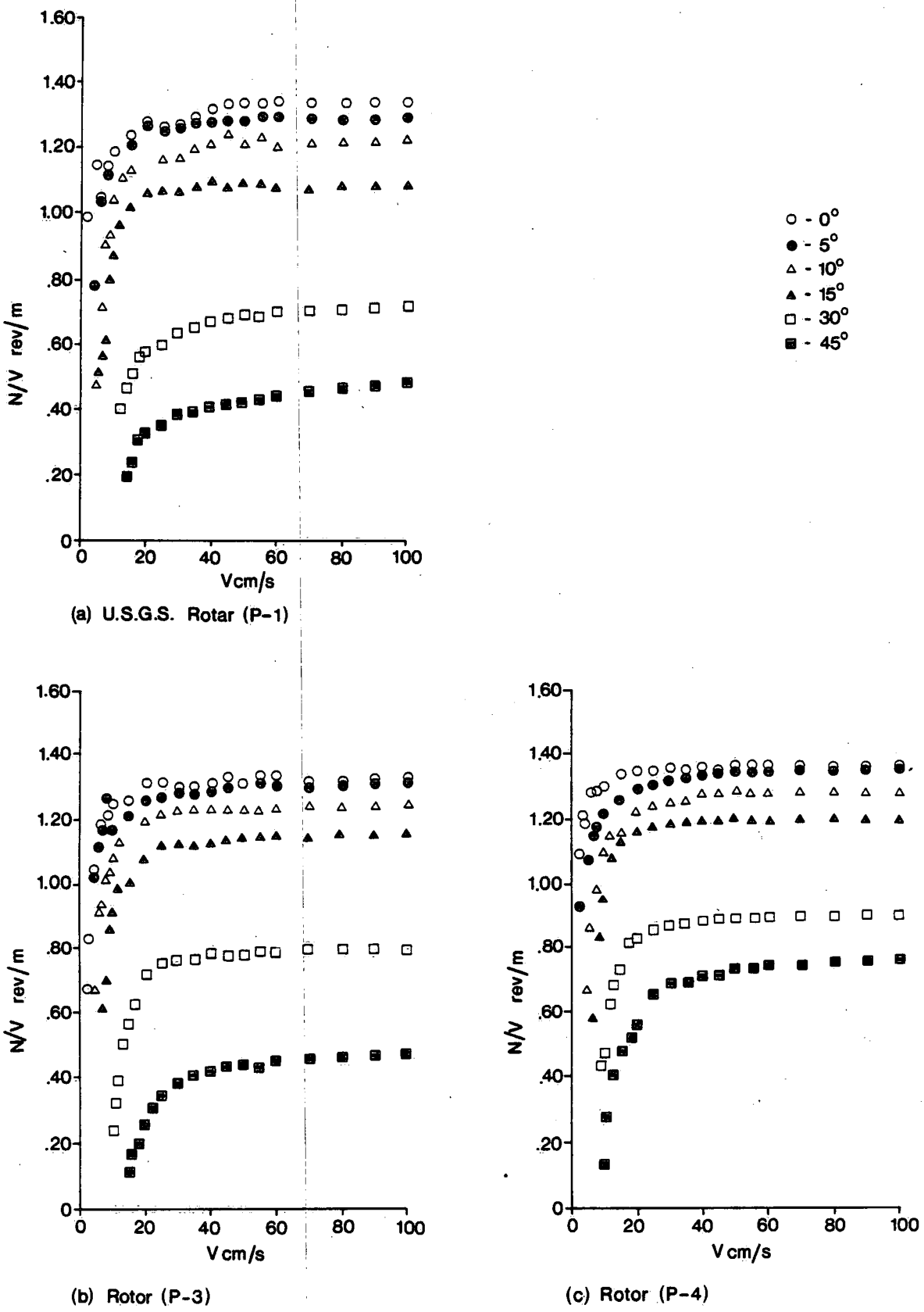

(a) U.S.G.S. Rotar (P-1)

(b) Rotor (P-3)

(c) Rotor (P-4)

Fig. 8 ROTOR RESPONSE FOR METER ANGLES ABOVE THE HORIZONTAL PLANE

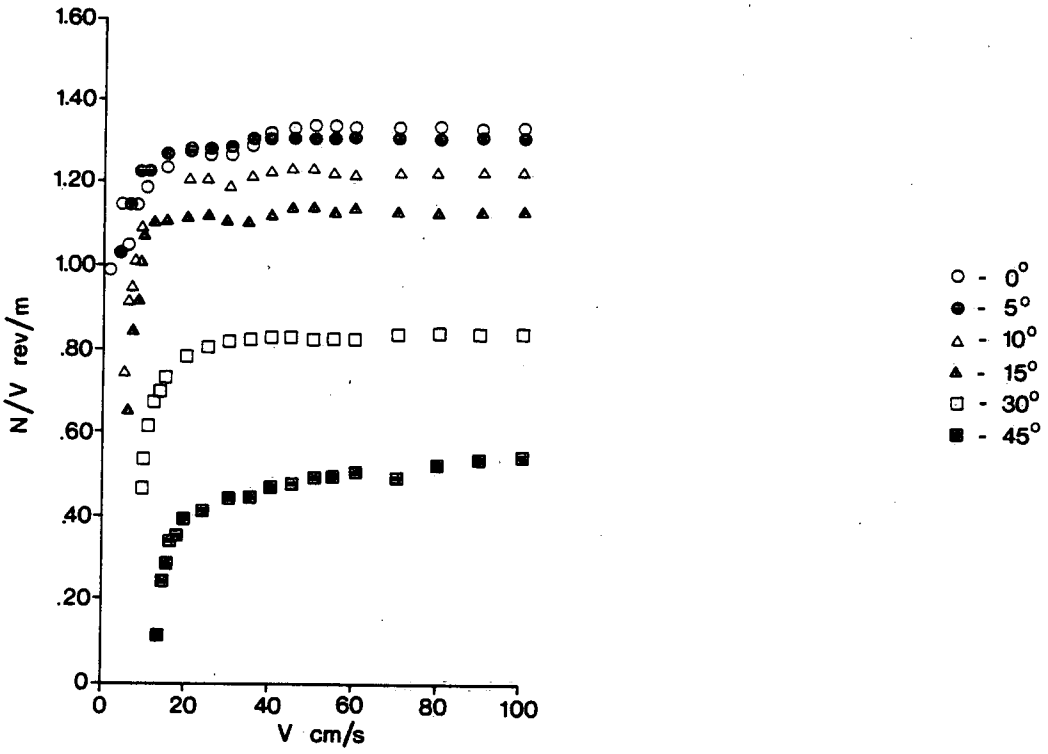

(a) U.S.G.S Rotor (P-1)

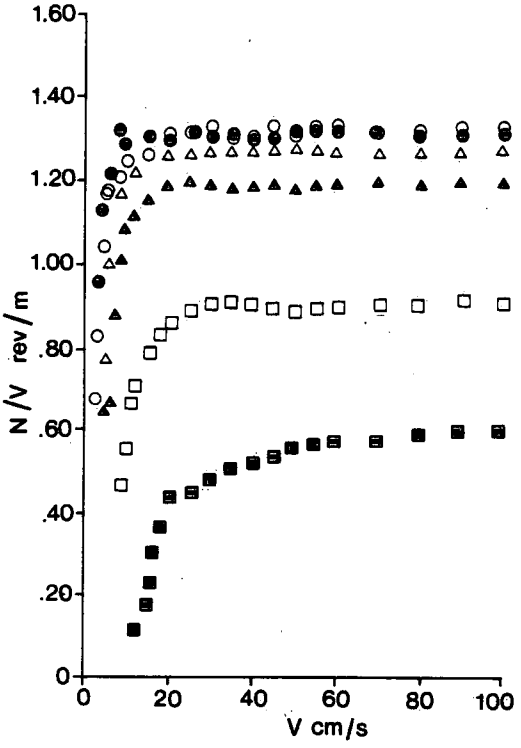

(b) Rotor (P-3)

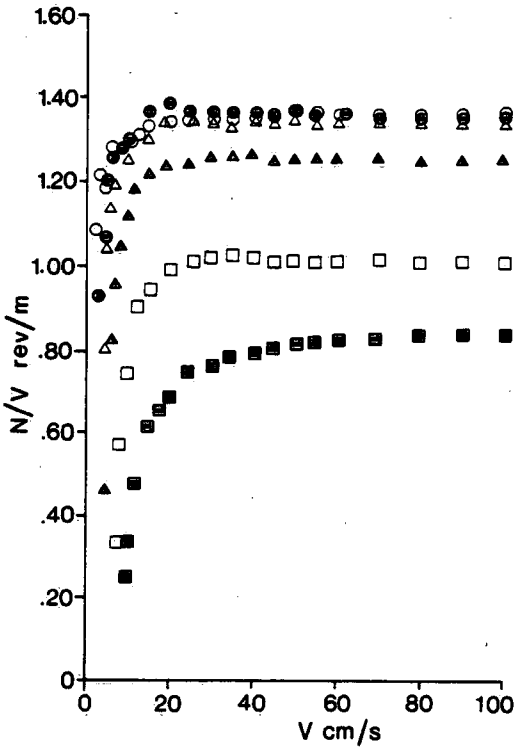

(c) Rotor (P-4)

Fig.9 ROTOR RESPONSE FOR METER ANGLES BELOW THE HORIZONTAL PLANE.